CONF-9607166--1

UCRL-JC-125157
PREPRINT

Modeling of Gun Barrel Surface Erosion: Historic Perspective

Alfred C. Buckingham

This paper was prepared for submittal to the
Sagamore Workshop
Wilmington, DE
July 29-31, 1996

August 1996

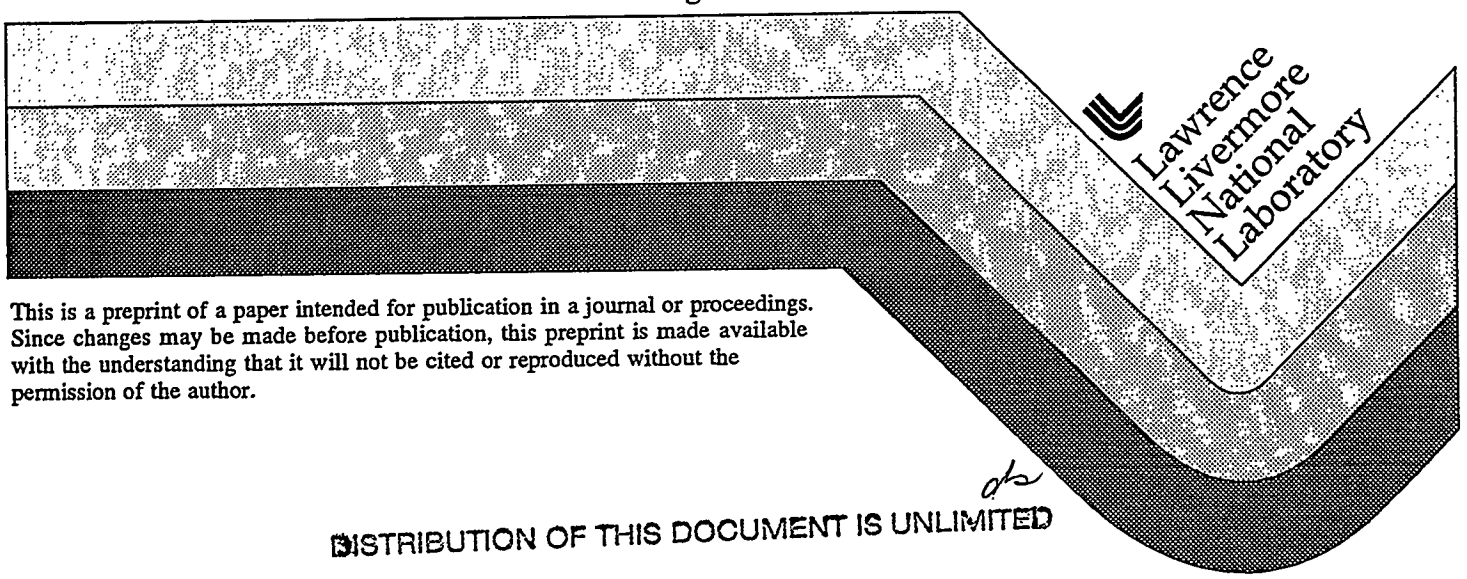

Modeling of Gun Barrel Surface Erosion: Historic Perspective *

Alfred C. Buckingham**
CENTER FOR ADVANCED FLUID DYNAMIC APPLICATIONS
H-Division, Physics & Space Technology Directorate
Lawrence Livermore National Laboratory, University of California
Mail Code L-17, P. O. Box 808
Livermore, California 94551

---

*Work performed under the auspices of the U.S. Department of Energy by Lawrence Livermore National Laboratory under Contract No. W-7405-Eng-48.

**Physicist, Fluid Dynamics, Retired Participating Guest Scientist.
Tel. 510-423-4828; Fax. 510-422-0966; Email. alfredcb@ocfkms.llnl.gov

Abstract

Selected results and interpretations of numerical modeling simulations of some dominant physical processes influencing gun barrel propellant combustion and flow-induced erosion will be presented. Results include modeled influences of erosion reduction techniques such as solid additives, vapor phase chemical modifications, and alteration of surface solid composition through use of thin coatings. For the purposes of this discussion emphasis will be placed on developing useful interpretations and predictions about erosion processes by modeling and evaluating the influences of dominant physical mechanisms and their dynamic evolution during the ballistic cycle. Attention to the identification and characterization of the numerical procedures, themselves are purposely avoided in the presentation, reserving specific comments on these aspects for informal, off-schedule discussions as needed or requested. Precedents and historical perspective are to be provided with predictions from essentially traditional interior ballistics approaches compared with those developed by more contemporary concentrated use of generalized, all-dominant process inclusive computer simulations. Consideration is given to the influences of: accelerating reactive combustion flow; multiphase and multicomponent transport; flow-to-surface thermal, momentum, phase change, and gas/surface chemical exchanges; surface and micro-depth subsurface heating, stress and composition evolution and their roles in inducing surface cracking, spall, ablation, melting and vaporization. Recognition is also given tocyclic effects of previous firing history on material preconditioning. Current perspective and outlook for the future are based on results of a purposely comprehensive U.S. Army - Lawrence Livermore Lab erosion research program covering about seven years of effort beginning in the late 1970's These results are supplemented by more recent research results on hypervelocity electromagnetic projectile launcher performance in selected cases where physical and scale similarities together with conditional parallels exist.

OUTLINE

I. Introduction

- Brief historical comments
- Small-scale, near-surface perspective

II. Statement

- General physical description
- Model simplifications, peculiarities, and caviats.

III. Predictions, observations & interpretations

- Damage phases
- Additives
- Material considerations - coatings

IV. Summary & projections

- Erosion reduction possibilities & drawbacks
- Modeling Advances

This is an outline of my discussion with you today. I begin with a short introduction consisting of a few historical comments on erosion prevention practices and early modeling attemps followed by my focus and emphasis on near-surface influences. I emphasize the barrel wall flow boundary layer or flow gap couette layer of the order of a few hundred microns to perhaps a mm thick in large calibre guns and the adjacent solid barrel erosively influenced surface layer of the order of 10's of microns. I follow with a few comments on the physical problem statement and some peculiarities about the restrictions or caviats associated with modeling this region. Then I will present some model results and some experimental observations covering some of the damage phases of significance in gun erosion and some tests and interpretations of some erosion alleviating procedures such as additives, coatings and propellant flow control. I will finish with some pros and cons about these procedures and some conjecture about the direction that modeling may take in the future. Since this talk is intended as a historical review, I have added an alphabetic reference list at the end which is identified in the text with authors' initials and publication date. Many of my remarks are based on our Lab's participation in an Army sponsored gun erosion research program beginning in the late 1970's and lasting until the mid 1980's (B-S-P-G, 83), (B-P, 84), (P, 84), supplemented by somewhat parallel research on electromagnetic (EM) propelled hypervelocity projectiles in rail guns. (B, 81b), (B-H, 82), (B-H, 90).

I. Introduction

- Brief historical comments
- Small-scale, near-surface perspective

In this introduction, I will make use of an almost canonical cartoon of the large calibre gun interior components to provide background for some history and some hints at my perspective and focus on the small-scale, high-gradient near-wall flow and sub-surface barrel layer. The figure follows immediately.

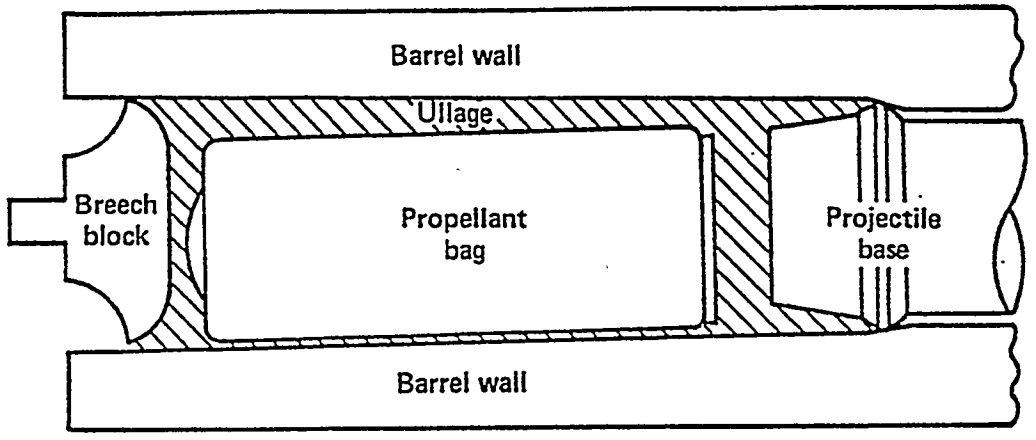

Here is the classic schematic, almost canonical sketch illustrating the basic interior features of large-calibre guns: the loading breech with a measured amount of propellant for the range and the purpose and the base of the projectile fitted at the start of the interior (often rifled bore). Early attention on gun erosion focussed on the heat of the propellant combustion, intensified by the pressure and vaporized combustion products on the interior bores of guns as exemplified by the use of cloth swabs dipped in convenient containers of sea water used to scavenge and cool the cannon bore interiors between firing rounds of ships cannon on early sailing men-of-war and the similar use of scrubs (sans water) to clear charring residue of land based ordnance. The Twentieth Century saw initiation of attempts to model the heating to bore surfaces using simple, constant property correlation heating coefficients, pressure-acceleration dependent constant density formulas, and other somewhat optimistically hopeful "fits" of complicated near-wall processes. (C, 50). More substantive analysis of the near wall convective heating environment awaited application of modeling approaches of sufficient resolution to describe the steep energy, momentum, and species concentration profiles in the neighborhood of the wall surface. For gun barrels this demanded development, extension and application of multispecies, multiphase component boundary layer solutions appropriately adjusted for propellant combustion composition and flow environments. Our physical problem statement serves as an introduction.

II. Statement

- General physical description
- Model simplifications, peculiarities, and caviats.

We move here to a statement of the physical problem and some model simplifications, peculiarities and restrictive assumptions we must keep in mind when we are interpreting results or using the model to design or assist in experiments.

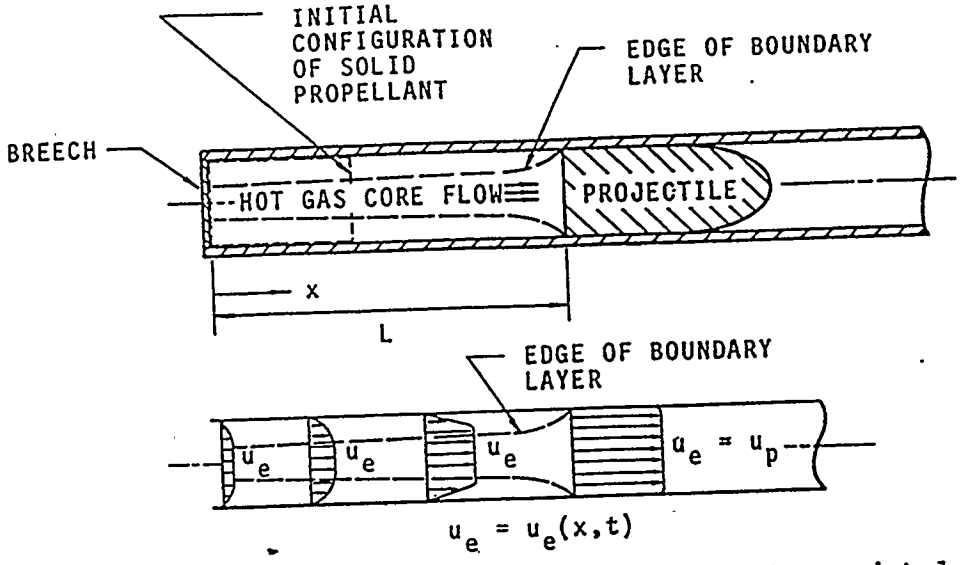

Schematic of Gun Barrel and Associated Velocity Profiles

This schematic indicates the in-bore growth of the boundary layer from its zero thickness origin at the base of the advancing projectile and diminishing again to zero thickness at the propellant bed. The basic point is that the boundary layer characteristics change with space and time throughout projectile acceleration and must be treated with this generality, if they are to yield useful information on heat and mass transfer, concentration of species and debris or additives concentrations. When the in-bore projectile has accelerated to a sufficient speed the influence of the projectile motion no longer significantly influences the pressure field between breech and projectile base, although this is not true at start-up of projectile motion which requires a different, more mathmatically elaborate treatment for valid results (S, 64). This start-up problem receives considerable separate attention here as it is associated with the time interval and location of the most significant erosive damage.(B, 79), (B, 80) In this division of problems, the second problem treatment begins after significant projectile motion with the acceleration modeled by single family characteristics methods for unsteady boundary layer solutions (B-A-K, 72), (B-S, 81), (B, 81a), (B-S, 82).

Definitions - thin fluid surface layers

- Here we make the distinction between boundary layers and Couette layers
- The former develops at the surface in the plasma behind the projectile
- The latter forms at melt or vaporization between armature and barrel walls
- The latter concerns us in the solid armature surface analysis here
- Important facts about thin layers:

  They do not support a pressure gradient → p(top) = p(bottom)!

  The velocity profile gives us the shear. The energy profile gives us the transfer. Shear and heat transfer are analogous & proportional.

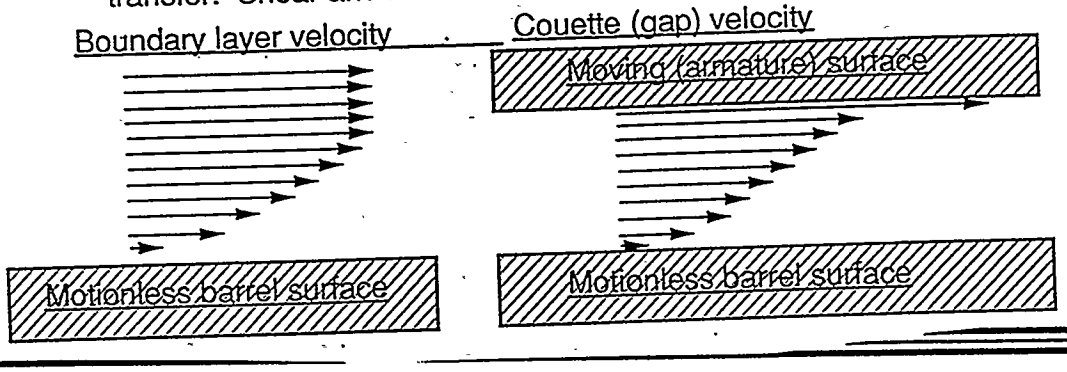

This schematic illustrates the basic simplification used in defining thin layer flows. These are thin enough so that the miniscule distortion to the momentum field can be neglected. This neglect permits spatial simplification of the general Navier Stokes equations, and replacement of the inertial driving terms with exterior boundary conditions. We obtain very high resolution of transport and species information by attention to a very narrow region of the flow, exclusively. We also illustrate Couette flow which results when erosive melt creates a film layer gap between moving projectile and the stationary barrel wall, a phenomena that often occurs in very high speed EM projectile launch (B, 81b), (B-H, 82), (B-H, 90).

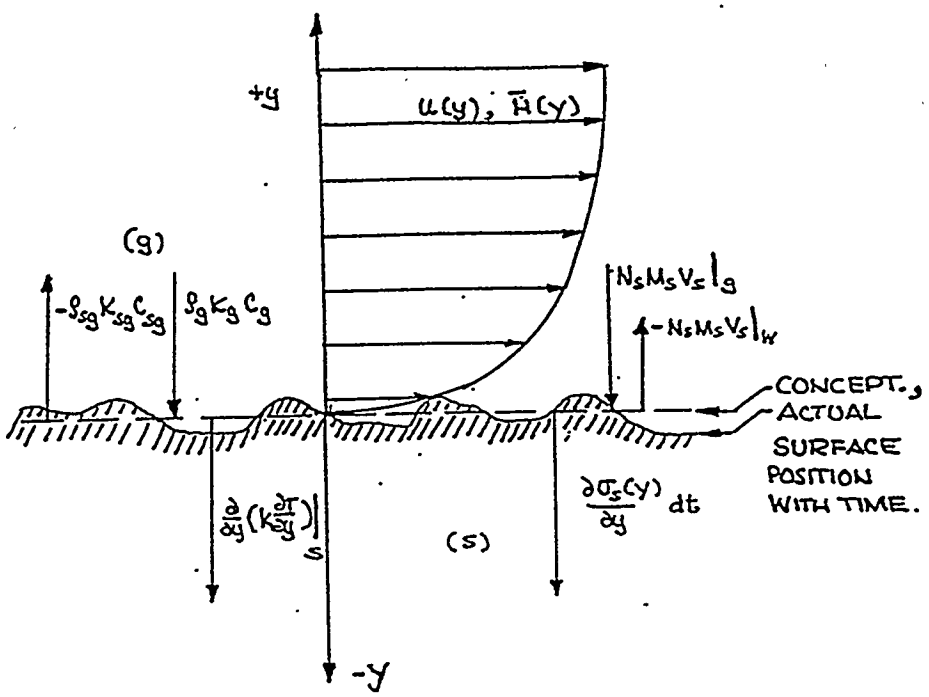

This sketch represents the conceptual modelled energy balance between the hot, debris-particle laden boundary layer on top and the eroding wall surface on the bottom. On the left, at the top in the "gas" (g) region we have the thermal film exchange in internal energy between gas (g) and solid (sg) components; while into the solid, from the hot gas moves the incident heat flux in Fourier conduction, to the right below the boundary layer is the thermal stress change in time associated with the Fourier heating of the solid, while above is the mass flux of impinging gas phase debris particles (g) and the opposing mass flux of eroded solid particles (w).

MIXTURE CONTINUITY

Global

$$\frac{\partial \bar{\rho}}{\partial t} + \frac{\partial}{\partial X_j}(\bar{\rho}\tilde{U}_j) = 0 \text{ , assumption } \frac{n_p m_p \langle U_p \rangle}{n_g m_g \langle U_g \rangle} \ll 1$$

time-averaged expanded sums:

$$\phi(t) \Rightarrow \rho, p, \tau_{ij}, q_j \cdot \quad \bar{\phi}(t) = \phi_g(t) + \phi_p(t) - \phi'_g(t)$$

$$\bar{\phi}(t_0) \equiv \frac{1}{2\Delta t} \int_{t_0 - \Delta t}^{t_0 + \Delta t} \phi(t)\, dt \quad \text{and} \quad \bar{\phi'}(t) \equiv 0.$$

mass-averaged expanded sums:

$$\Phi(t) \Rightarrow U_i, H, h, I \quad \tilde{\Phi}(t) = \Phi_g(t) + \Phi_p(t) - \Phi''_g(t)$$

$$\tilde{\Phi}(t_0) \equiv \frac{\overline{\rho(t_0)\Phi(t_0)}}{\bar{\rho}(t_0)} \quad \text{and} \quad \overline{\rho\Phi''} = 0 \quad \text{but} \quad \bar{\Phi}'' = \frac{\overline{\rho'\Phi''}}{\bar{\rho}} \neq 0 !$$

Species

$$\frac{\partial(\bar{\rho} m_\ell)}{\partial t} + \frac{\partial}{\partial X_j}(\bar{\rho}\tilde{U}_j m_\ell) - \frac{\partial}{\partial X_j}\left[\bar{\rho} D_\ell^T \frac{\partial m_\ell}{\partial X_j} - j_\ell\right] = \psi_\ell$$

$D_\ell^T = D_\ell$ (Molec) + D_ℓ (Turb) ; ψ_ℓ (Net production rate of ℓ specie).

The next two figures illustrate the formulation of the continuum multicomponent, kinetically reactive, multiphase equations of motion for turbulent propellant flow, written here in Cartesian repeating tensor notation for convenience and transformed with appropriate metrics (B-S-L, 60) for the geometries to which they are applied (cylindrical symmetry for the gun tube). The boundary layer formulation is based on that originated by Kendall and Bartlett for laminar chemical equilibrium flow (K-B, 68) and extended to the second phase of unsteady turbulent gun tube flow later (B-A-K, 72). Moment coefficients are based on classic statistical mechanical collision integral approximations to the Boltzmann-equation (H-C-B, 54), with linearization of the molecular exchange processes in Mason-Saxena form (B-S-L, 60). Chemical kinetic rate equation arrays for coupled combustion flow systems are based on several available sources including Edelman and Harsha (E-H, 77) as well as current combustion work at Sandia (Hardesty et al) and at the LLNL (Westbrook, Pitz, et al.). Briefly, the equations are developed for wall layers in conjunction with special asymptotic considerations and constraints on the energetic coupling between viscous boundary layer influences and kinetics (B-F, 77). The first figure illustrates that we must add the influence of species continuity to that of continuum continuity and for compressibility we must consider both mass and time averaging to develop the appropriate field averages for turbulent flow. A dimensionally consistent correction for sparse particle loading is also shown.

MIXTURE MOMENTUM AND ENERGY

Momentum

$$\frac{\partial(\bar{\rho}\tilde{U}_i)}{\partial t} + \frac{\partial}{\partial X_j}\left[\bar{\rho}\tilde{U}_j\tilde{U}_i + \Theta\delta_{ij}p - \Theta\left(\bar{\tau}_{ij} - \overline{\rho U_i'' U_j''}\right)\right] = 0$$

$$\Theta \equiv \frac{v_g}{v_g + v_p}$$

Energy

$$\frac{\partial(\bar{\rho}\tilde{H} - \bar{P})}{\partial t} + \frac{\partial}{\partial X_j}\left[\bar{\rho}\tilde{U}_j\tilde{H} + \Theta\bar{q}_j + \overline{\Theta\rho U_j'' h''} - \Theta\tilde{U}_i\left(\bar{\tau}_{ij} - \overline{\rho U_i'' U_j''}\right) - \Theta\overline{U_i''\left(\tau_{ij} - \frac{\rho U_i'' U_j''}{2}\right)}\right]$$

$$- \frac{\partial}{\partial X_j}\left[\sum_{\ell}\left(\bar{\rho}D_\ell^T\frac{\partial m_\ell}{\partial X_j} - j_\ell\right)\tilde{h}_\ell - \frac{R\bar{T}}{\rho}\sum_{\ell}\sum_{m}\frac{\alpha_m D_\ell^T}{M_\ell D_{\ell m}}\left(\frac{j_\ell}{m_\ell} - \frac{j_m}{m_m}\right)\right] = 0$$

Mixture momentum and energy generalized formulations are illustrated in the next figure. Consideration is given to the transport approximation for systems in near-equilibrium composition states for the highly dissipative boundary layer regions using some elemental models (B-S-L, 60), but with a substantially developed basis in statistical mechanics for multicomponent systems (D, 62).

III. Predictions, observations & interpretations

- Damage phases
- Additives
- Material considerations - coatings

We move next to some modeling predictions, some experimental observations and some interpretations in our pursuit of understanding erosion processes. It is emphasized that in gun erosion, modeling and theory are interactively boot-strapped with experiment. The same is true for nearly all current physics experiments since experimental access and resolution are usually limited so that alternate (simpler) experimental configurations are used to fix certain carefully controlled parameters (usually well off-scale conditionally from the real situation). Simulations and modeling are used to link several such off-scale conditional observations and, in trials, to approach the real experiment for few controlled features are possible and diagnostic access is limited. New experiments are then devised to more closely approximate the real situation and to establish resolution requirements for diagnostics development and application. We discuss some erosive damage phases, the use and influences of erosive-suppressing additives, and some barrel surface material considerations and tests.

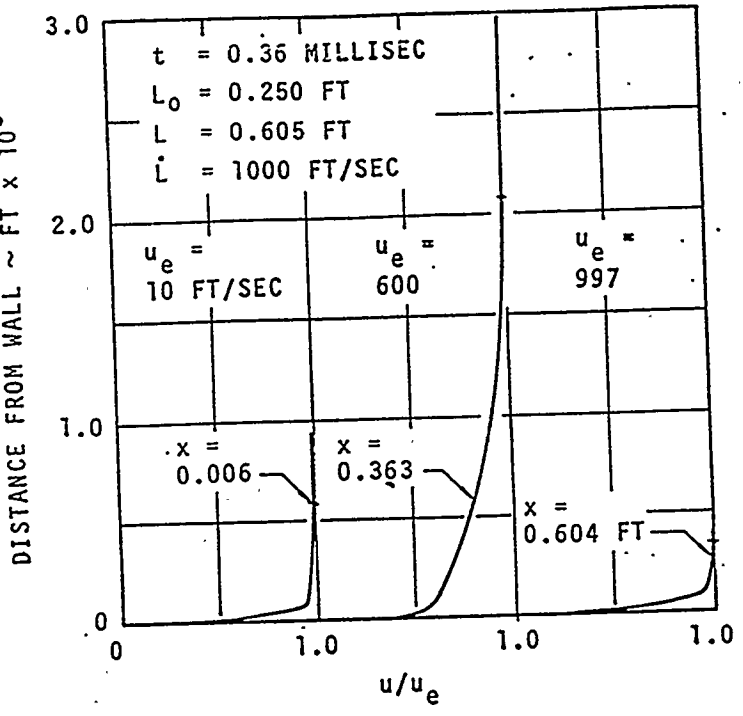

Turbulent Boundary Layer Profiles at Several Stations at a Given Time

This figure illustrates the dimensions of a growing turbulent boundary layer in terms of the velocity profile (ratioed to edge values) behind a projectile whose base has moved about 185 mm away from its original position about 75 mm from the breech. In this example calculation, at this time the boundary layer thicknesses are seen to increase from about 160 microns to a peak of 610 microns and decaying back down to less than 100 microns near the base of the projectile which conceptually is impulsively accelerated to just over 300 m/s constant velocity.

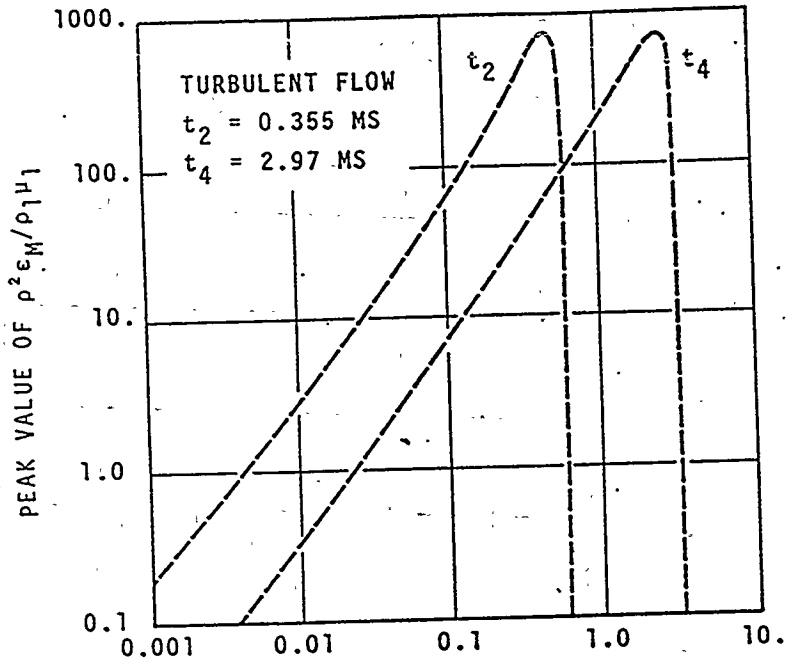

Peak Eddy Viscosity Along Gun Barrel for Several Times

Some estimate of the intensity of turbulent shear (and by analogy heat transfer) compared to that of laminar flow are given in the next figure which shows ratios of turbulent eddy viscosity reaching values nearly 1000 times their laminar counterpart for the same flow conditions. More recent experiments and theoretical results show increases about one order of magnitude greater than the ratios depicted here.

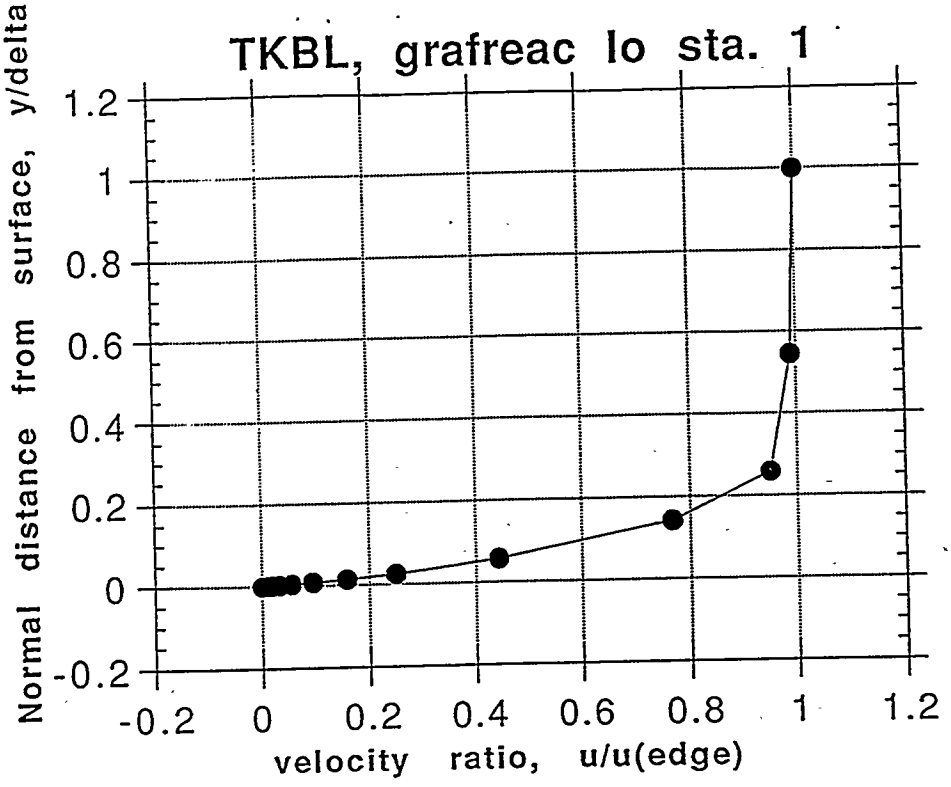

An expanded view of the boundary layer velocity profile(ratioed to the outer edge value) is given next in the calculated results for a gun station near the origin of rifling at an early time when the projectile base has moved about 3 bore diameters away from its rest position.

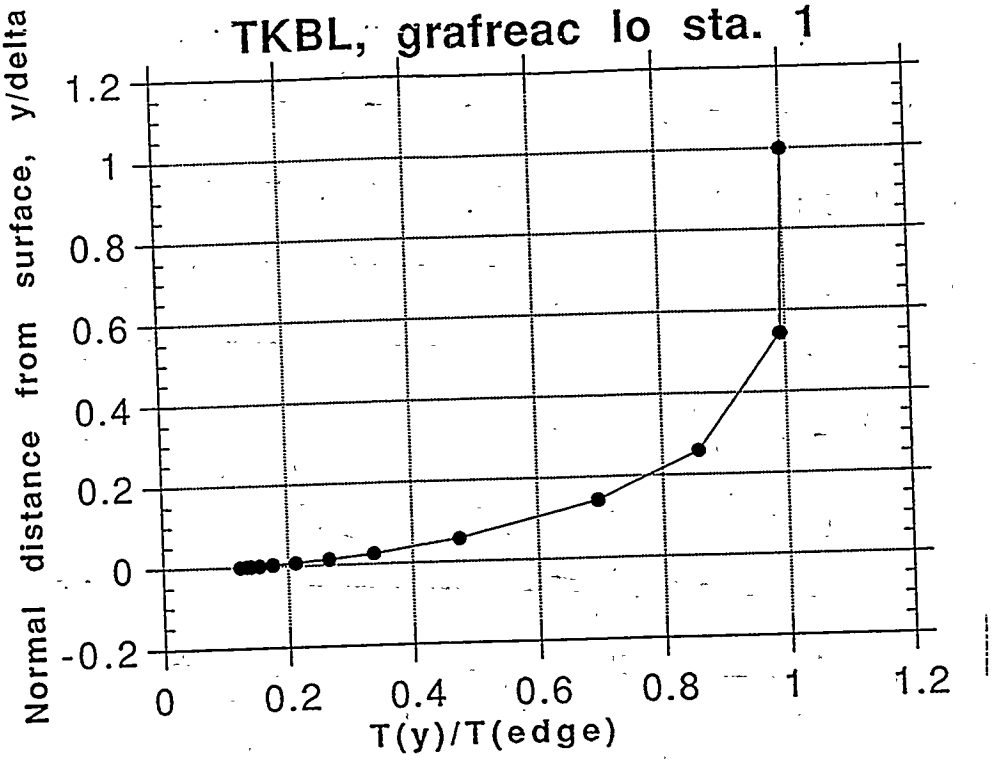

The corresponding sharp temperature gradient at the same position and time as the previous figure are illustrated by the modelled results in the next figure. Here, the similarity seen between velocity (shear) and temperature gradients are manifest indications of the applicability of Reynolds analogy which suggests direct proportionality in these quantities.

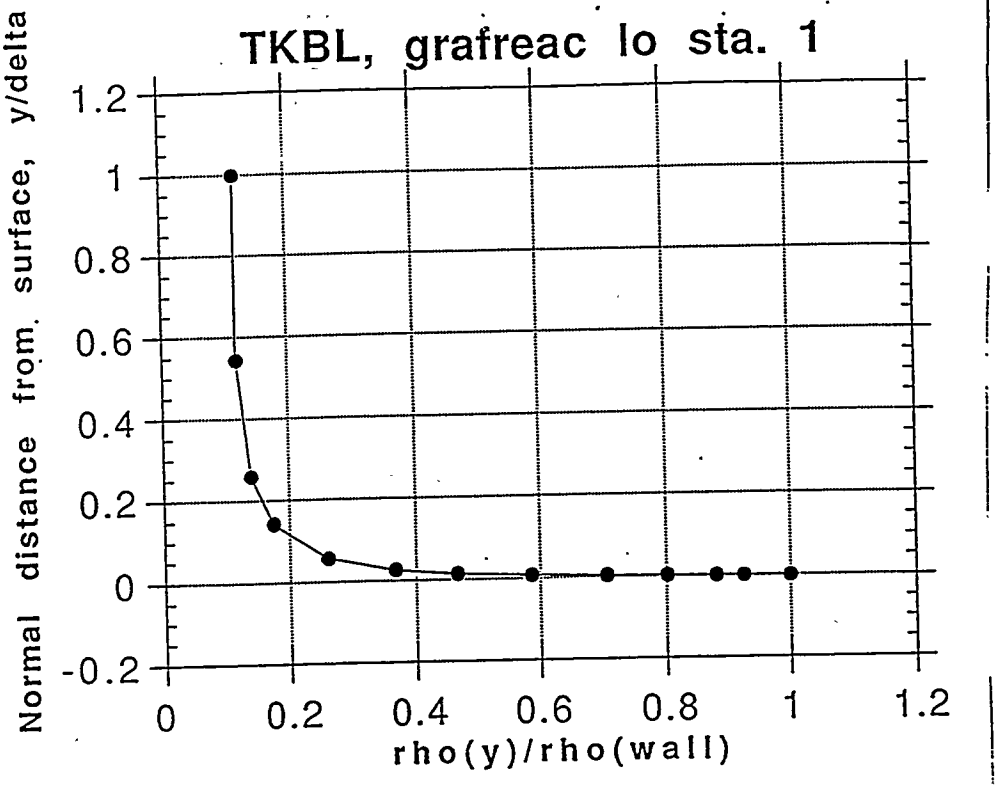

In this next figure, the turbulent mean density profiles at this same station and time, indicate the fallacy of the use of a constant density model as was done in some earlier gun tube heat transfer predictions for what is now recognized as the fully compressible flow wall boundary layer of a gun tube.

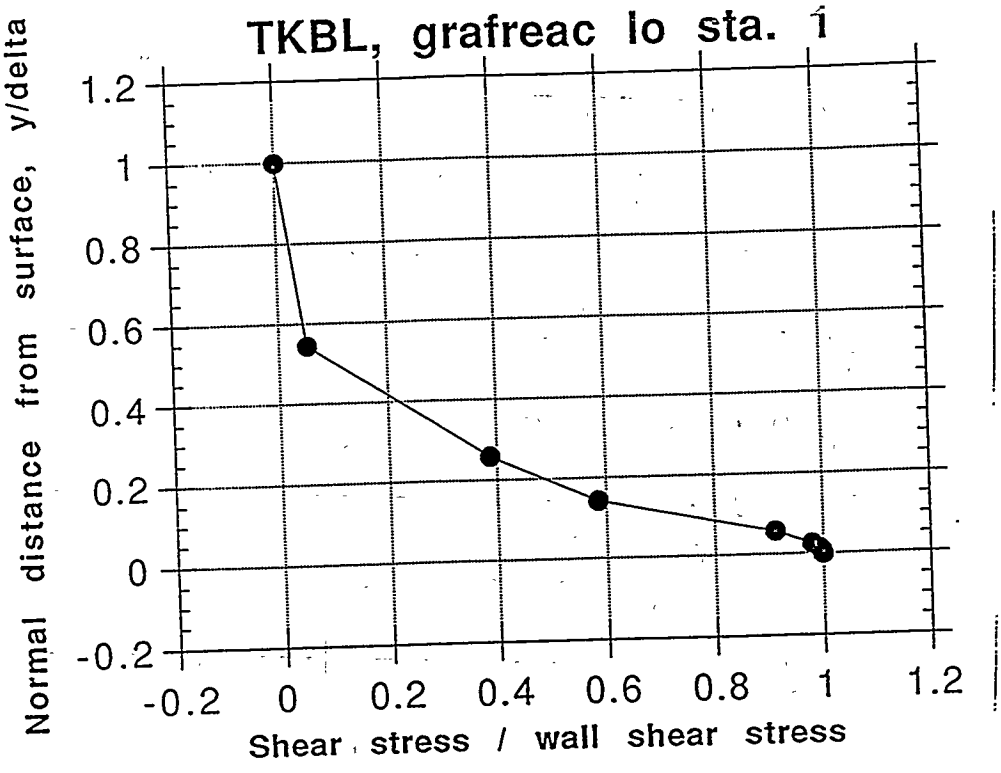

Again at the same spatial location and time as the previous figures, the steep build-up of turbulent shear stress in the boundary layer as the barrel surface is approached is illustrated in this figure.

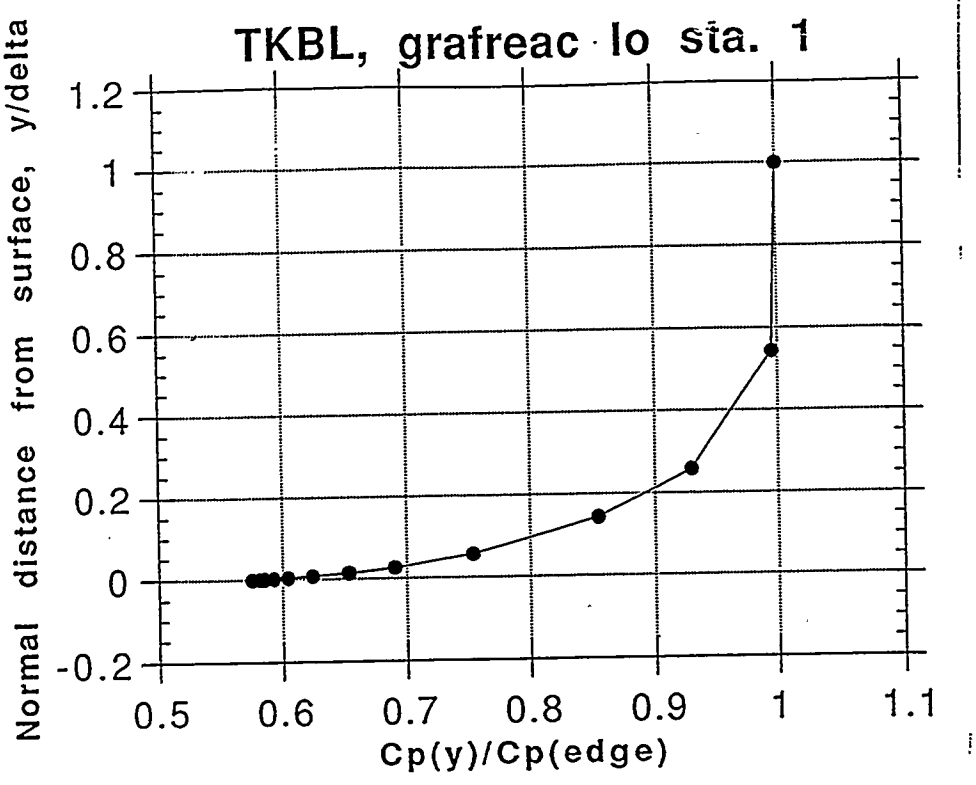

The thermodynamic and transport properties which strongly influence the heat and mass transfer rates at the wall in the multicomponent turbulent boundary layer also illustrate the fallacy of relying on constant property coefficient based heat transfer correlations for gun tube predictions as was the practice some years ago. This figure illustrates the orders of magnitude fall-off in gas phase component averaged constant pressure heat capacity as the relatively cool barrel wall is approached.

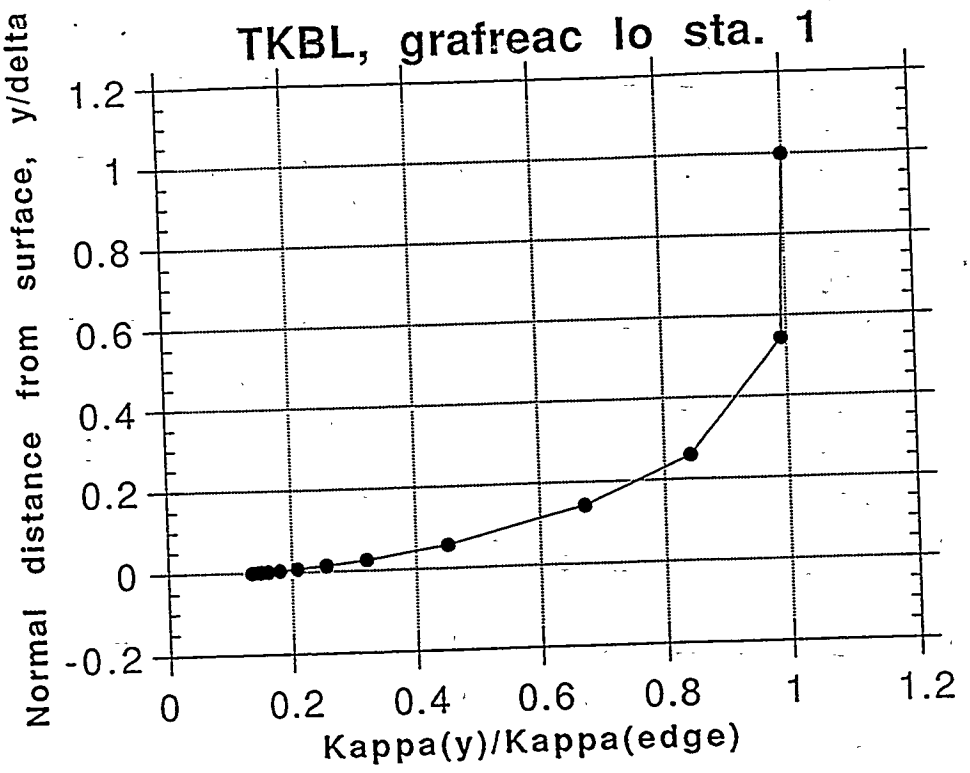

The ratio of gaseous boundary-layer component-averaged thermal conductivity to the hot propellant flow value at the outer edge of the boundary layer and the steep gradient to a vanishlingly small relative value near the cool wall are illustrated in this figure.

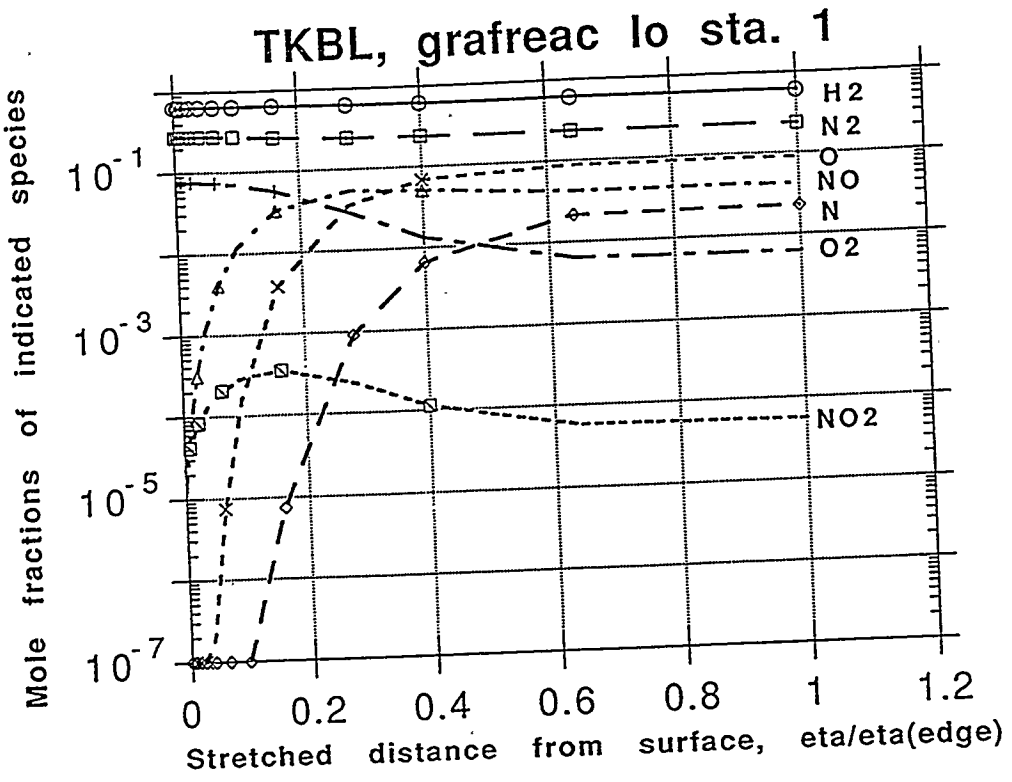

In the next figure, we illustrate the influence of wall injection and transpiration cooling in modifying the severely erosive heating environment associated with our experimental electromagnetic rail gun propulsive system research. (B, 81b), (B-H, 82), (B-H, 90). Here the chemically reactive turbulent boundary layer for intensely heated real air behind the advancing electromagnetically driven projectile was modeled with our boundary layer code driven by core flow boundary conditions from a separate set of modeled plasmadynamic solutions. In the present case modest amounts of hydrogen gas are injected from insulator ports in the EM barrel wall to ascertain the effectiveness of light gas injected transpiration cooling. Steep gradients appear in the predicted dissociative recombination of Nitrogen-Oxygen argon free air model species profiles as the cool wall is approached from the hot core flow. The projectile was moving supersonically in these cases with launch velocities of from 4 to more than 6.5 km/s. The Hydrogen gas diffuses rapidly from the wall in an inert, non-reactive state with relatively substantial enhancement of the cold wall heat capacity near the wall for cooling.

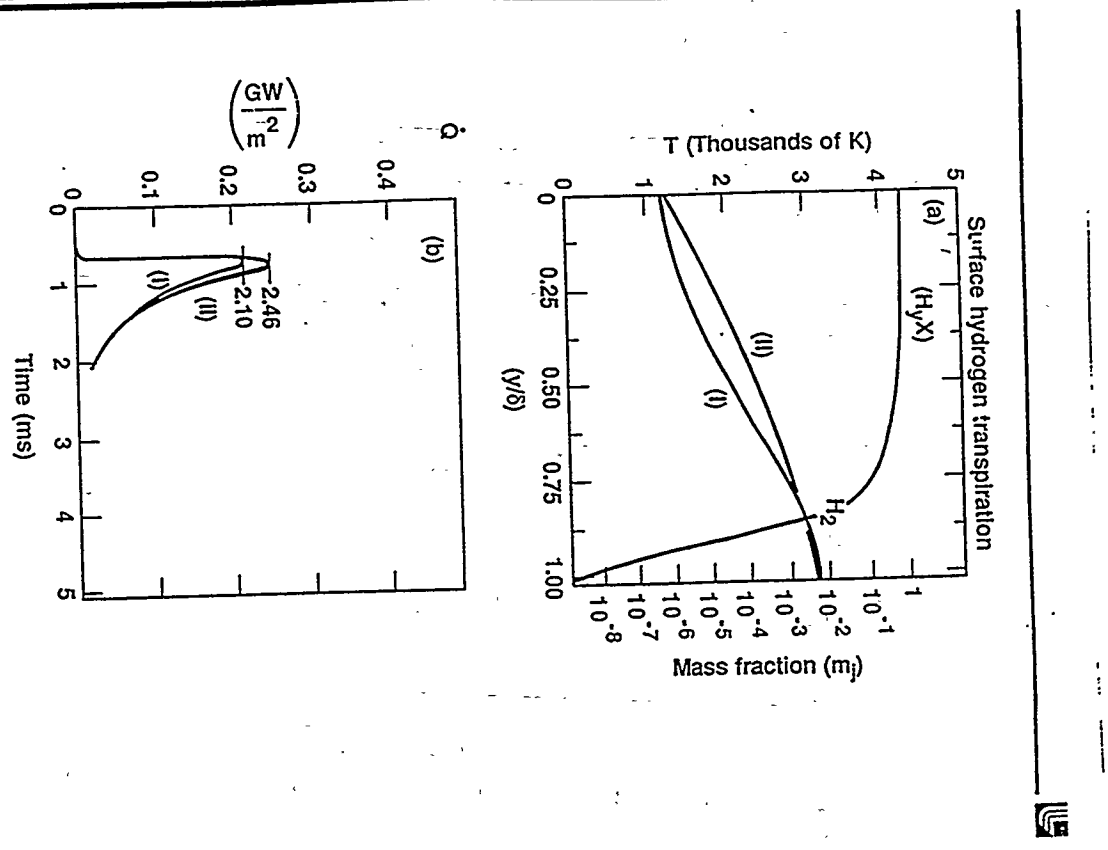

The next Figure at the top shows the core-to-wall mixture temperature distributions without Hydrogen injection (I) and with Hydrogen injection (II). The bottom Figure predicts an almost 18% drop in peak heat flux to the wall at a fixed position associated with the Hydrogen secondary injection.

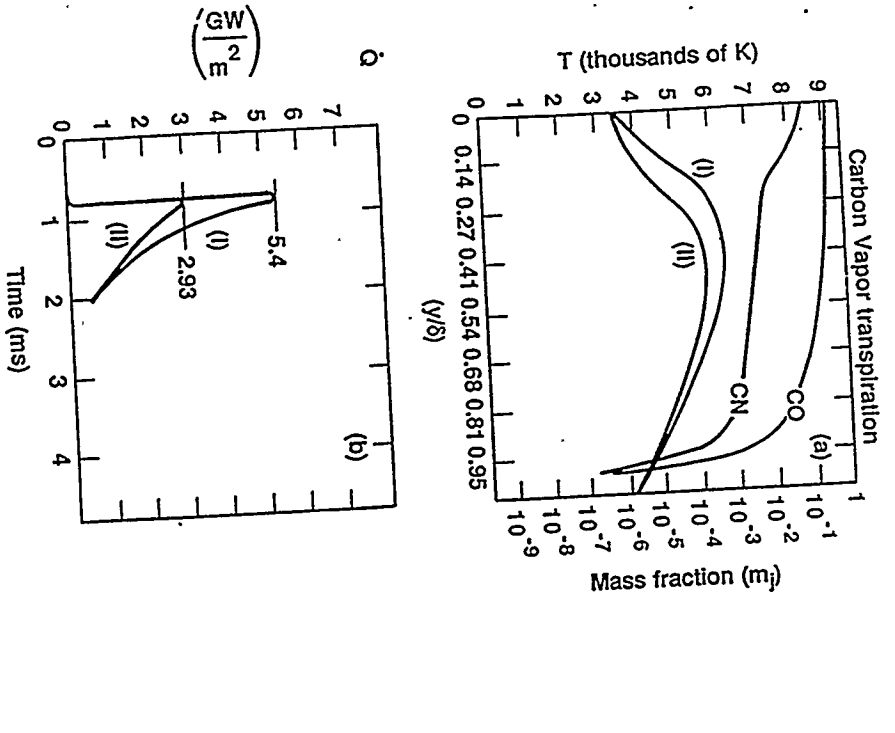

The next figures depict modeled results for transpiration cooling of reactive CO and CN injected in the wall region of the boundary layer at the same position as the foregoing inert Hydrogen injection case. Here the heat flux at the wall is reduced substantially more in association with the endothermic dissociation reactions of the carbonaceous compounds. The predicted drop in peak delivered wall heat flux is about 45% using the reactive compounds at a favorable injection point.

PURPOSE OF MIXTURE/SOLID STATISTICAL SIMULATIONS

1. Influence of "dust" distributions on transport, state
2. Energy partition
3. Kinetics: gas, gas ↔ surface, surface
4. Interface layer and substrate micro → macroscopic changes

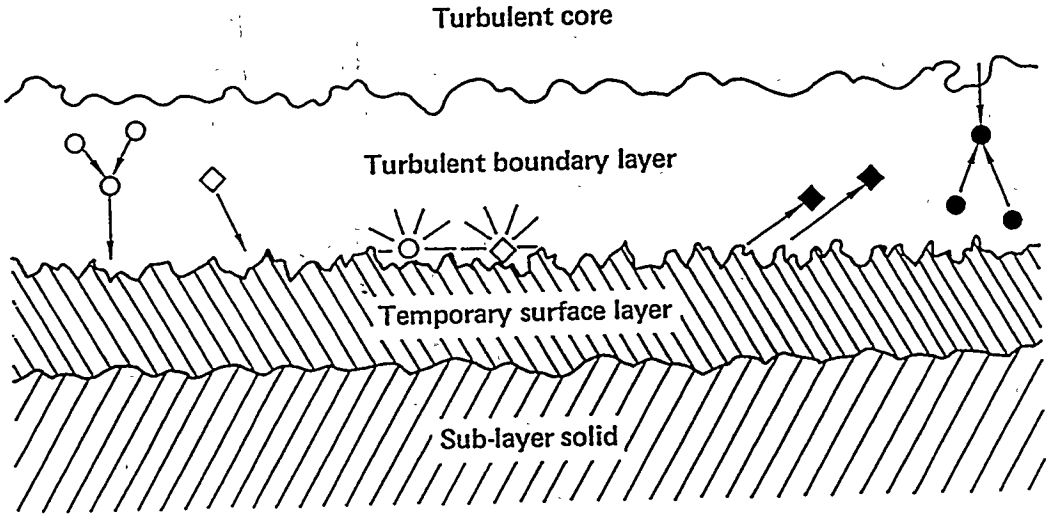

We next move to modeling the influence of erosion-suppressing solid particle additives such as talc, TiO2 and SiO2, among others which have been suggested as candidates for erosion reduction in previous studies. (F-L-S, 79), (G-D-A, 55), (H, 70), (P-T, 72), (R, 75). In our studies we developed and utilized a stochastic, Monte-Carlo based model procedure involving up to 10,000 target particles limited to binary collisions. The model calculations simulated trial realizations for turbulent particle dispersion and distribution as well as attempts later to check on the back influence of turbulent gas particle loading on damping turbulent intensity, hence reducing heat and mass transport. This first schematic illustrates the conceptual picture of turbulent flow borne particles and their influence on the barrel wall surface. Our studies emphasized the importance of particle mobility in interacting with the erosive propellant flow rather than simple passive non mobile changes to gaseous heat capacity, a concept which had been followed extensively by some previous investigators.

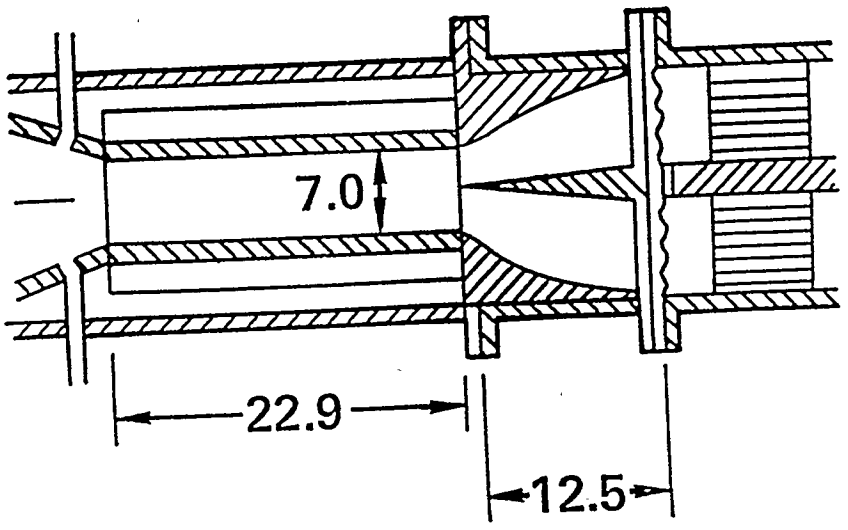

In addition to developing and testing this stochastic model, design, test and definition/interpretation of two different sets of related experiments were conducted in a combustion tube at the University of California, Berkeley (B-S, 82), (B-S-E-D, 83), (B-S, 83) and in dusty-gas shock tube facilities at the University of Southampton, in the U.K., and at Australian National University. (B, 85), (B, 86), (B, 87). Experimental design, diagnostics, and development of the stochastic model found incentives in earlier work (C-P, 72), (Y-C-A-U, 77). The heart of the Berkeley experiments was the use of a splitter plate to divide two parallel streams of different density which form in a mixing layer behind the splitter plate with provision for initiating combustion in the upper or lower sections (or neither). The schematic shows the test section with plane, optically transparent high-pressure windows for optical access. All dimensions are in cm units.Laser doppler anemometry was the primary diagnostic with the additional provision for particle sampling, collection and dispersal size distribution measurement.

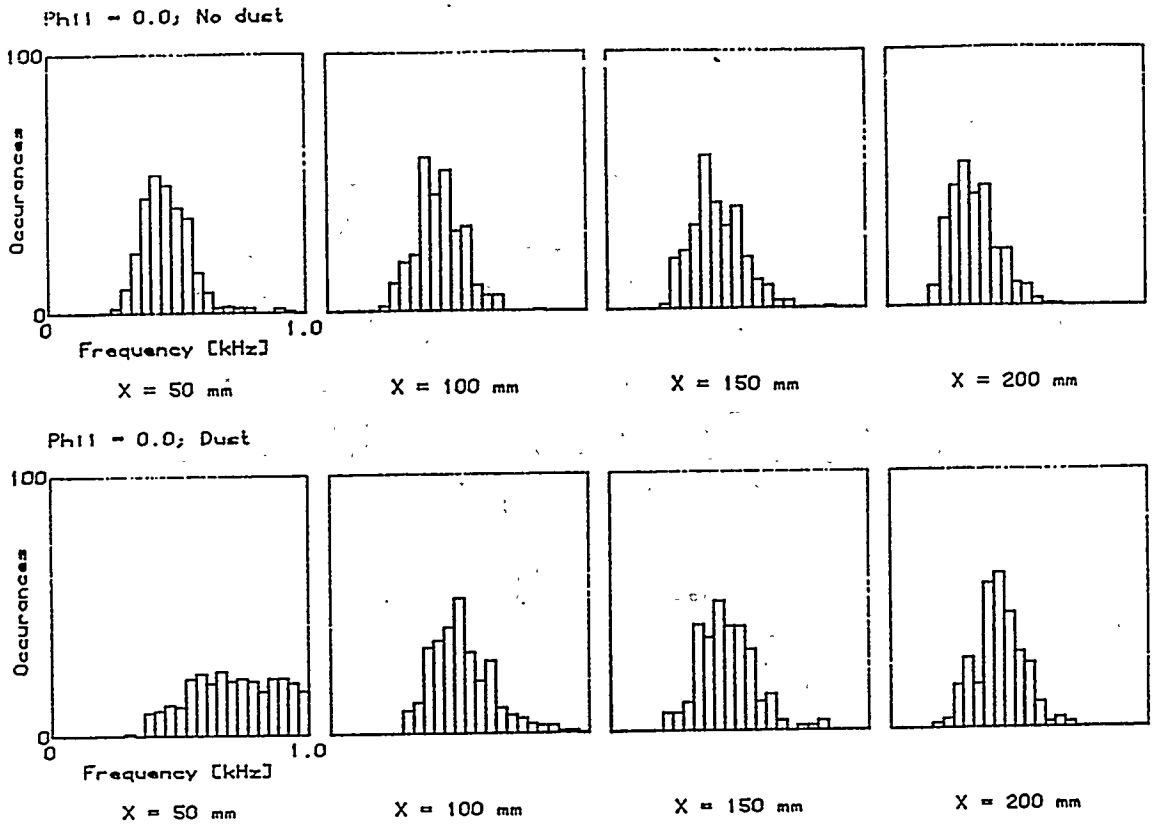

Some of the most dramatic demonstrations of the influence of dust particles on turbulent flow are shown in these U. C. Berkeley experiments on the mixing layer characteristics measured behind the splitter plate. These histograms measure the occurence of vortical motions in a particular size range, largest to the left moving to smallest sizes at the right. The largest motions carry most of the random mixing energy and are seen to be most effected (reduced) by the presence of fine scale dust particles (order of 1 micron mean diameter TiO_2 particles) close to the splitter plate (within 50 mm downstream) as shown in the lower row of pictures. Little influence is seen at larger distances where the fine dust is dispersed to densities too low to effect the apparent turbulent energy mixing spectrum in the production range.

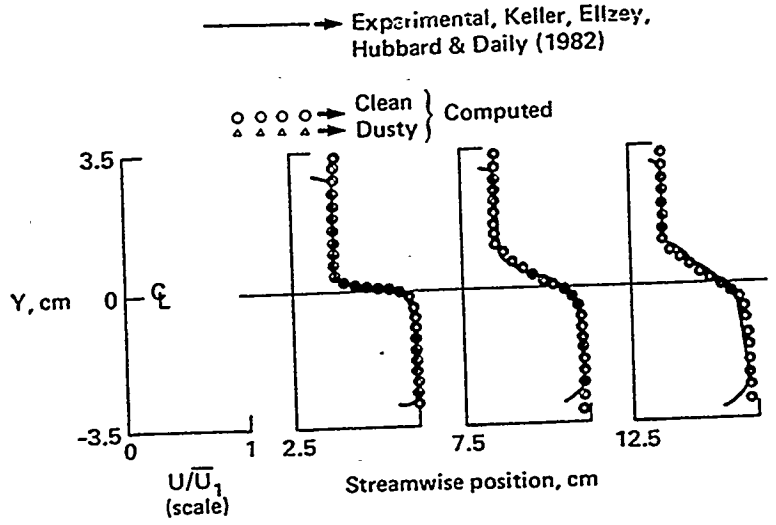

Mean flow profiles downstream from splitter plate, channel flow.

As seen in this illustration, particles have little influence on the mean flow. This is a set of profiles at various stations downstream of the splitter plate. The profiles are distributions of the mean velocity from bottom to the top of the test chamber. The experimental mean is the solid line, while the open (clean flow) and closed (additives present) symbols are ensemble averages of the full Monte-Carlo simulations taken over a sampling of realizations once the turbulent field had developed nearly stationary statistics. The particles have little apparent influence on the mean flow, effecting only the random components. The upper and lower wall regions are ill-defined by the Monte-Carlo LES model, hence separate boundary layer modeling for transport resolution was dictated for our research in this all-important erosive problem region.

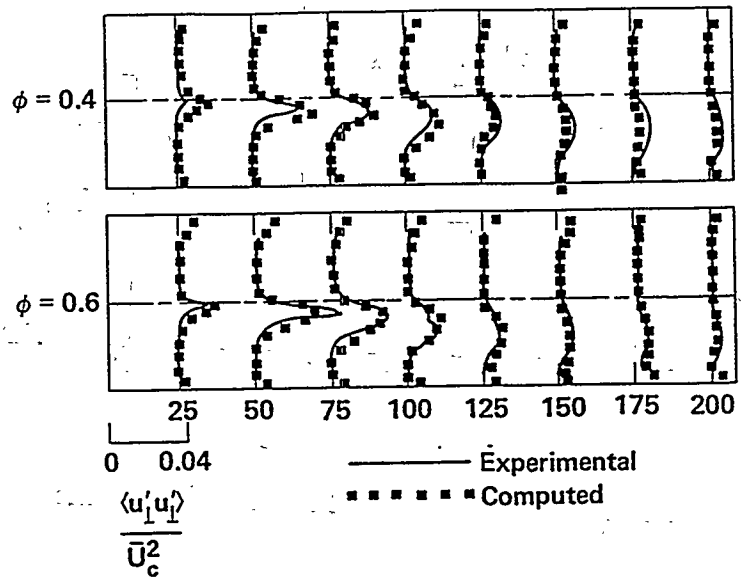

This illustrates the mean turbulent kinetic energy profiles from bottom to top in the test chamber at several stations behind the splitter plate. The simulations for additive laden flow are represented by ensemble averages of at least seven realizations. These appear as the solid symbols while the experimental results are averages over time of several instantaneous distributions and are shown as the solid line. The flow in both upper and lower frames is undergoing combustion. The parameter, ϕ, is the equivalence ratio, where unity is a stoichimetric mixture of oxidizer and fuel and 0. represents the all-oxidizer no-fuel limit. Again, the boundary layer region near the walls requires a separate modeling effort for usefully accurate resolution.

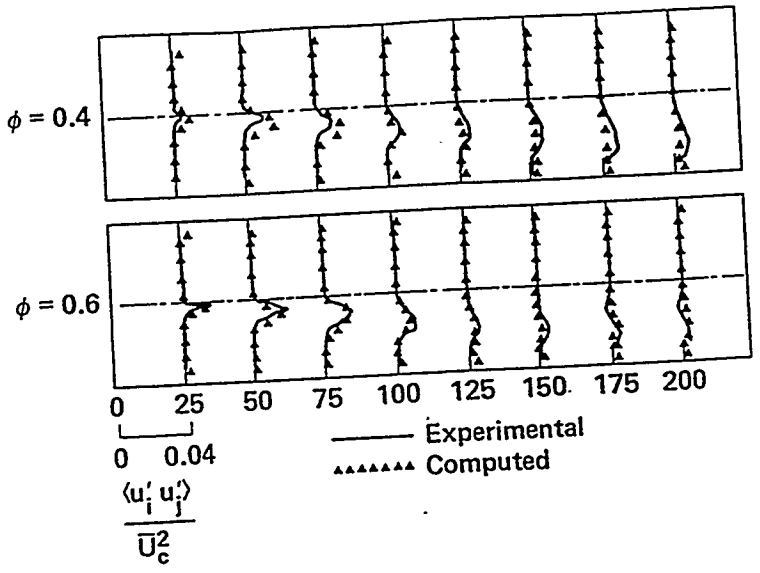

This picture illustrates the Reynolds stress distributions from top to bottom of the test chamber for simulated (symbols) and experimental (solid curve) averaged profiles at the indicated stations (the units are cm.) downstream of the splitter plate. The equivalence ratios of the two combustion flow field experiments are identical to that of the previous plot with the leanest combustion results represented in the upper frame. Again the simulation results are reasonably accurate except in the region of the wall where separate boundary layer resolution is required.

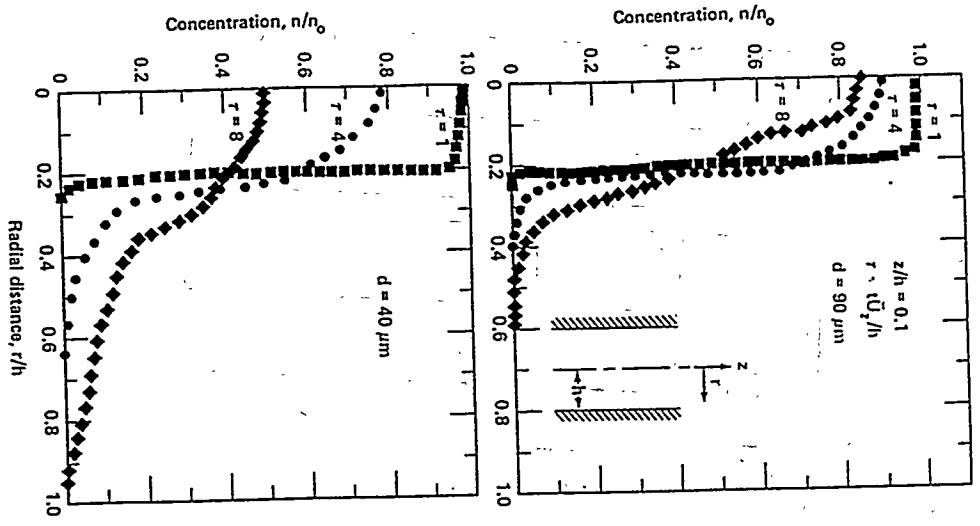

Use was made of the Monte-Carlo LES model to simulate particle dispersal in a turbulent flow from a variety of initial additive particle positions in a chamber. The effect of particle size on the dispersal is shown in this figure where the initial position for all of the test particles is within a virtual cylindrical boundary occupying 20% of the half-width, h, of the modeled cylinder. Random dispersal for the smaller (40μm) particles is seen to provide almost twice the radial distribution in comparison to the larger (90μm) additive model particles.

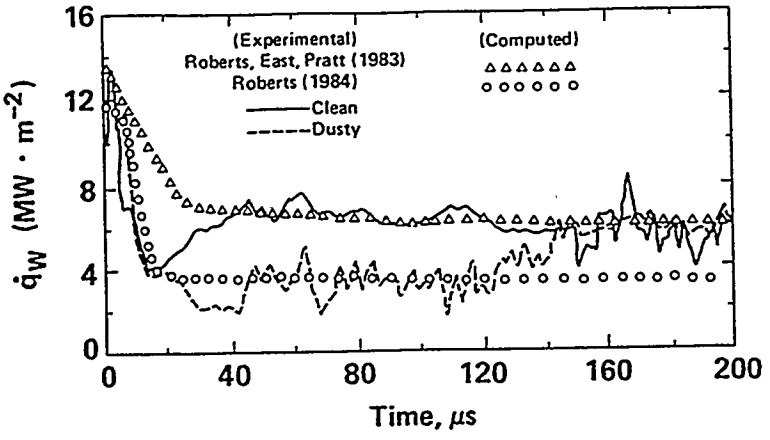

Kinetically inert gas phase, shock tube

To develop and test the boundary layer model for turbulent reactive flow with additives, we developed a collaboration with an experimental shock tube research effort in compressible dusty gas flow and heat transfer at the University of Southampton and at Australian National University. (B, 85). A Mach 5 shockwave was initiated in non-reactive argon for one set of tests. A reactive mixture of CO, CO_2, and H_2 in argon diluent was used for the reactive flow tests. Additive dust was entrained from an initial distribution by the advancing shock wave boundary layer intersection at the wall. Heat transfer and pressure measurements were continuously recorded from rapid response thin film surface heat transfer gages mounted flush with the base plate. In this first figure both clean flow and additive laden flow results of the boundary layer solutions are shown as symbols superimposed on the gauge traces shown as a solid line. These results for non-reactive flow are usefully close to the experiments except near the end of the dusty gas experiments (when the dust from the reservoir was exhausted).

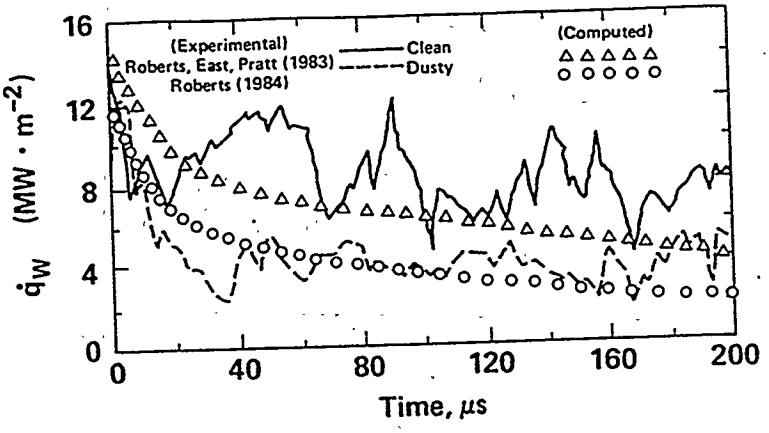

Reactive gas phase, shock tube

For the reactive flow, however, the experimental results, particularly for the clean flow exhibit considerable additional structure, not reflected in the relatively smooth boundary layer averages. The trends were appropriate but the lack of detail in the local temporal structure in the model clearly points to a difficiency in time averaged continuum behavior for simulating this type of important flow. This is a clear call for added attention to development and test of a large eddy simulation sub-grid scale model with an accurate treatment of the near-wall limiting solutions.

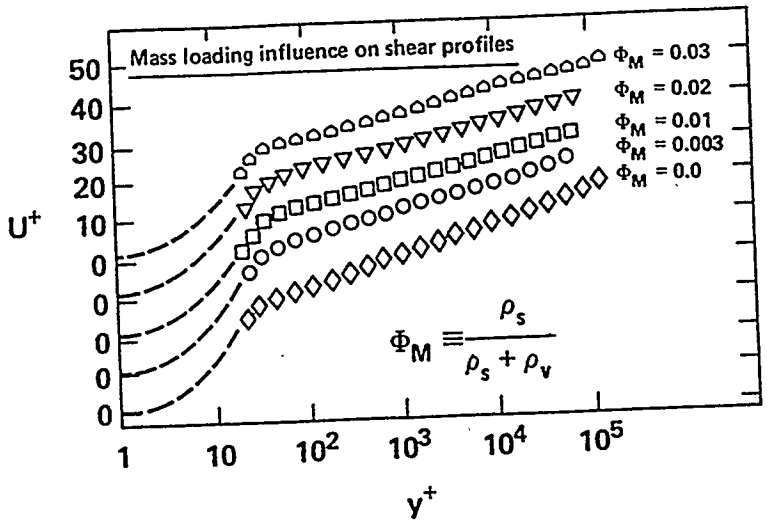

Continuing with the dusty turbulent boundary layer analysis of the effects of additives we examine the change in the turbulent shear as a function of dust loading in the near wall region of a cooled wall boundary layer. Only a small amount of dust dispersal in this region shows considerable influence on reducing the steepness of the velocity profiles, hence the shear. The velocity and normal displacement from the wall are given in wall variables, u+, and y+. The former is the ratio of the boundary layer velocity to the shearing velocity at the wall, while the latter is the square root of the product of the normal displacement and the shear velocity divided by the kinematic viscosity.

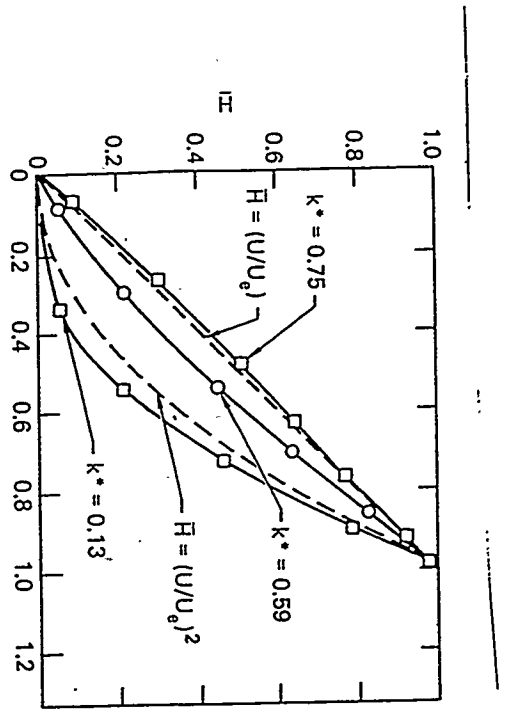

Fig. 10 Predicted effects of 0.3 μm particle loading on boundary-layer enthalpy profiles.

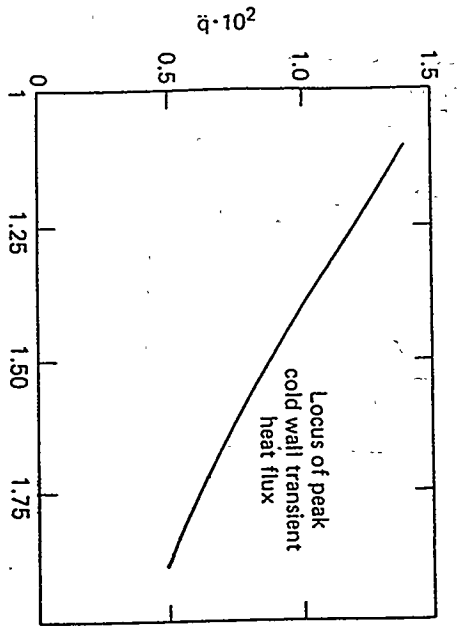

Fig. 11 Comparison of predicted effects of particle loading on cold wall heat transfer.

In the upper figure we illustrate the influence of particle additive loading on the steepening of the boundary layer enthalpy profile as a function of boundary layer velocity, where the parameter, k*, is 1. - particle mass density/gas mass density, the lowest values representing the highest particle loading and largest influence on reduction of the steepness of the enthalpy profile slope and by implication the boundary layer work dissipated in the form of heat at the wall. In the lower figure we plot the average of several trials on the reduction of cold wall boundary layer heat transfer as a function of dilute particle loading. In the lower figure, the abcissa is the loading parameter, 1 + k*.

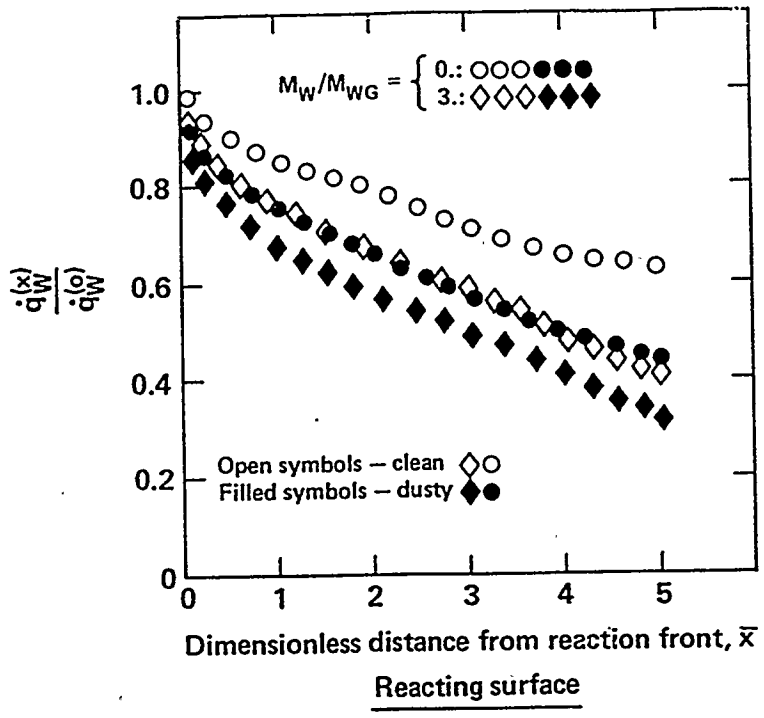

In the next two figures we illustrate the use of the turbulent reactive multicomponent boundary layer solutions in testing the affects of active wall to boundary layer reactions for additive laden dusty gas and for clean gas. The active wall is a model of reactive transpirant vapor coolant and of sacrificial (ablative-reactive) wall coatings. The first figure plots the decay of peak heating past the reaction zone.

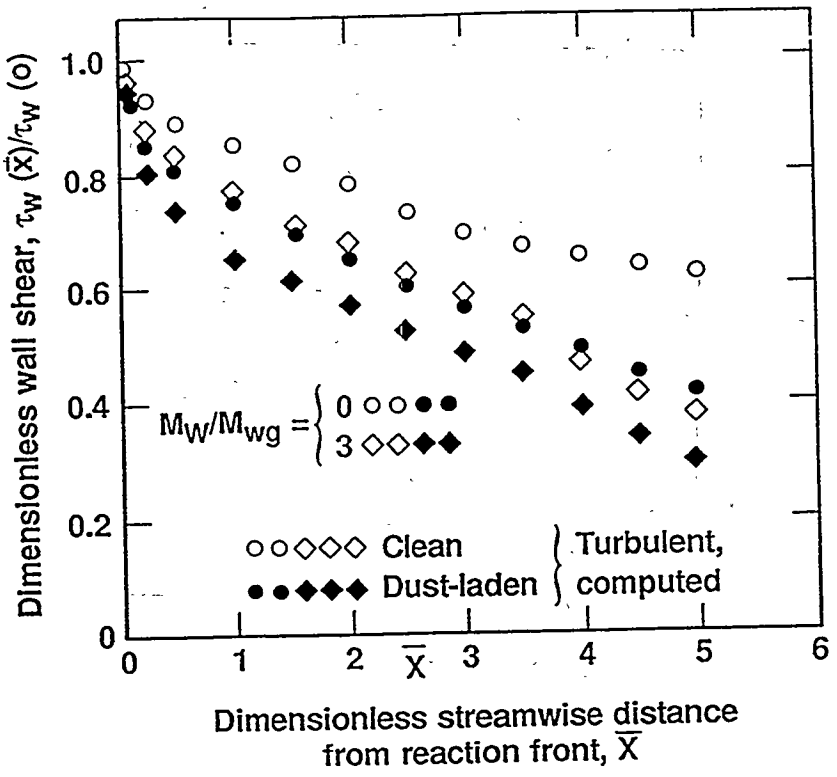

In this figure we test the influence of the reactive surface on reductions in wall shear for dust-laden and clean gas.

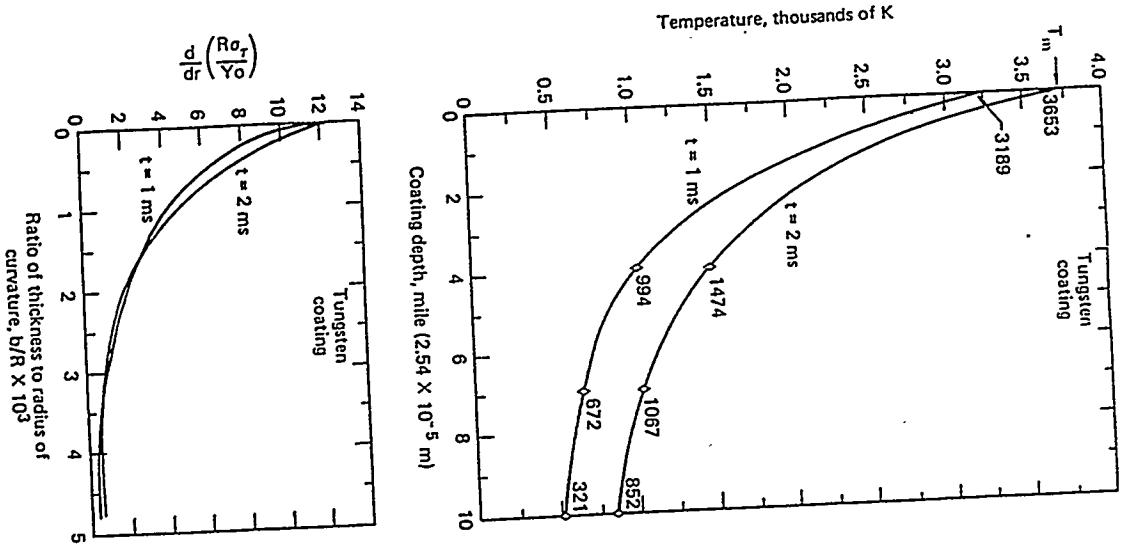

A variety of high temperature coating materials including amorphous (glassy) tungsten were evaluated using the dusty gas boundary layer model for surface heat transfer. In this figure we show the temperature profiles at two different times in sustained heat flux equivalent to the very high values associated with the peak pulses seen in our hypervelocity EM rail gun projectile launcher. The depth of coating is given in mils. The bottom figure plots the resulting dimensionless radial thermal stress gradient as a function of dimensionless coating thickness imposed on the tungsten coating. New experiments were designed. These used laser sustained-pulse interaction techniques on coating and substrate barrel material samples exposed to the laser pulses while contained in a sealed chamber filled with controlled concentrations of "propellant" vapor products. The model was used to define the more interesting material and vapor components and the appropriate diagnostics for in-situ and post shot experimental analysis.

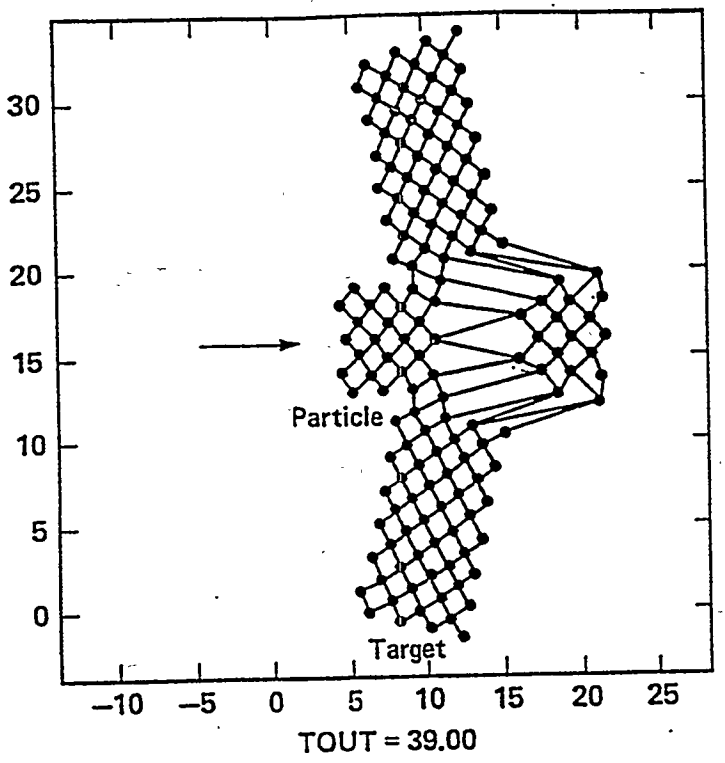

Particle-wall lattice dynamics collision and heat transfer simulation.

This figure illustrates an additional set of model calculations used to help determine the influence of propellant micro particle debris surface impact and molecular propellant vapor penetration on a variety of coatings. Shown in one such calculation of an 8 molecule thickness surface layer solid lattice with an impinging molecule. The influence of molecular speed, energy partition, mass penetration, and material surface damage are localized in these ab-initio molecular dynamics calculations. Experimental evidence from the laser interaction experiments in addition to theoretical macro continuum models (stochastic crack formation, ablation site probability distributions, energy partition, momentum accomodation) are used in conjunction with these ab-initio molecular dynamics results to develop continuum mechanics and statistical mechanics relationships and models relating these results to gun-tube environments.

IV. Summary & projections

- Erosion reduction possibilities & drawbacks
- Modeling Advances

We move here to our final discussion offering a summary and some projections.

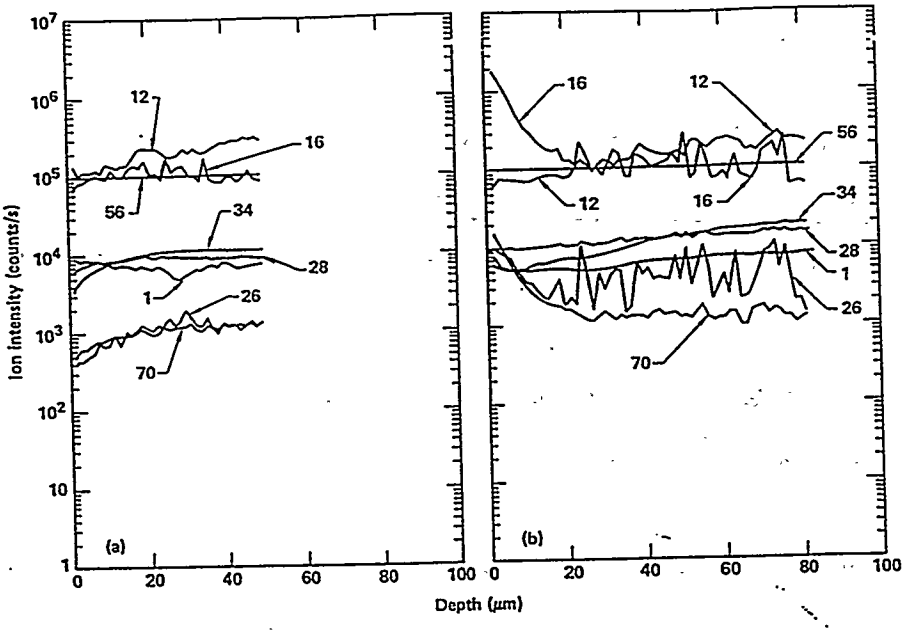

Figure 1

This figure and the next one illustrate the post laser exposure analysis of molecular penetration and in depth compositional changes that might occur for a variety of base metals and coatings in gun propellant environments. These are part of a large number of SIMS depth profile molecular analyses conducted on samples near the end of our Army program. (B-P, 84), (P, 84). Penetration and segregation of impurity atoms to the strain fields of coating dislocations and interstitial-dislocation interactions were under particular study. Mass isotopes examined included: H(1), C(12), O(16), [CN](26), Si(28), Fe(56), and [FeN](70). The numbers are labels to identify the isotopic profiles. The baseline sample (unexposed) is on the left. Exposure to a single laser shot in neutral argon yields profiles shown at the right. Of particular concern were the short range intensity profiles of C and of O.

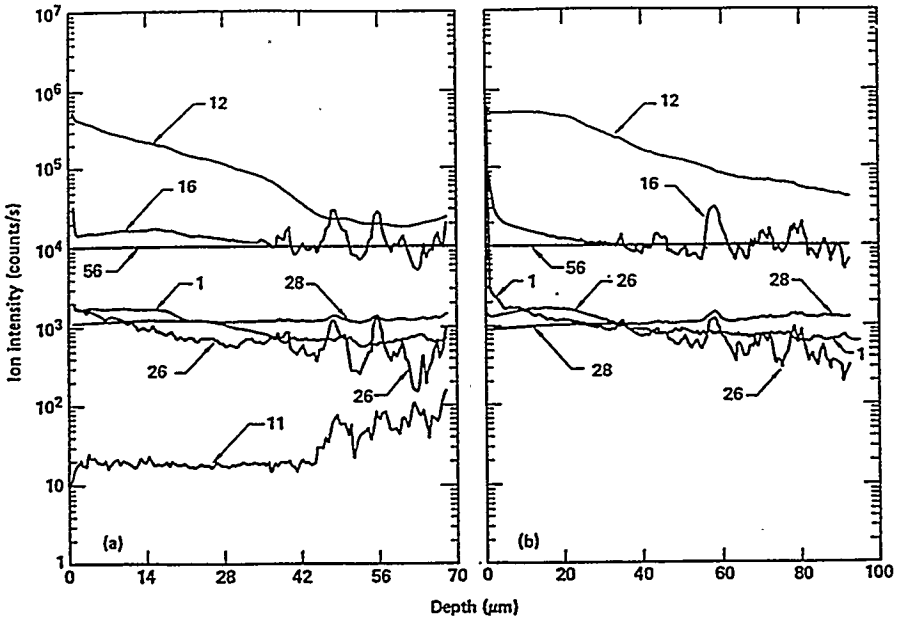

Figure 2

In this figure we see the results of laser pulsing in 10% methane, with argon as diluent at 10 atmospheres. The figure at the left received 10 pulses, that at the right 50 pulses from the laser. The persistence of certain dislocation features implies that much of the segregation-penetration-dislocation damage may occur at early stages in gun firing cycles. Thermal mechanical damage mechanisms may then proceed on repeated firing from a more or less fixed (albeit microscopically altered) compositional surface and sub surface structure.

Erosion reduction possibilities & drawbacks

- Inert & reactive particle additives
- Wall materials - coatings
- Propellant chemistry
- Passive initial acceleration plus: traveling charge, LP, EM... phase

We summarize here some erosion reduction techniques and some of the drawbacks to applying them in real gun environments. We discuss, in turn each of the bullet items.

- In many interesting flows the range of excited scales far exceeds that feasible for direct numerical simulation.
- Observations show that turbulent transport is carried primarily by the largest scale eddies.
- This is basis for hope that LES will suffice for practical computations.
- In LES the turbulence problem is reduced to treating the effect of the unresolved subgrid scales on those explicitly computed.

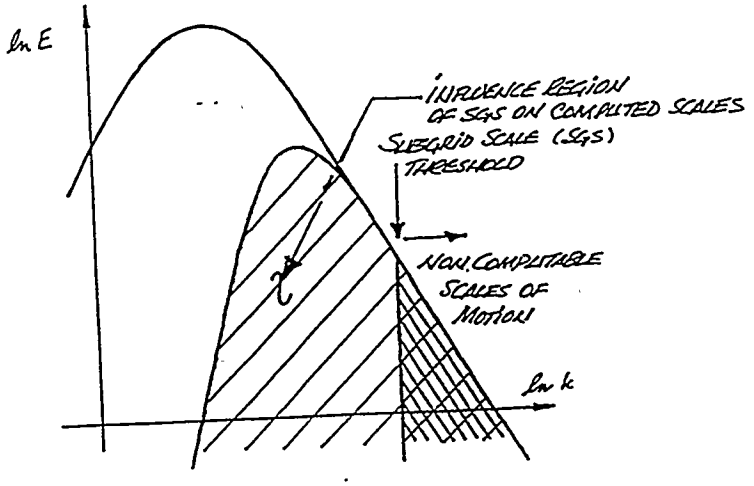

We move to projections on advancing in modeling techniques that we feel would be most useful in erosion and erosion reduction analysis for guns. Keeping in mind our emphasis on the near wall surface, we suggest a focus should be on developing generalized large-eddy-simulation procedures. The key is the sub-grid scale model that reproduces detailed information in the wall boundary layer in a combustion environment. In this figure we define the LES generally and suggest some of the obstacles which must (and will) be overcome.

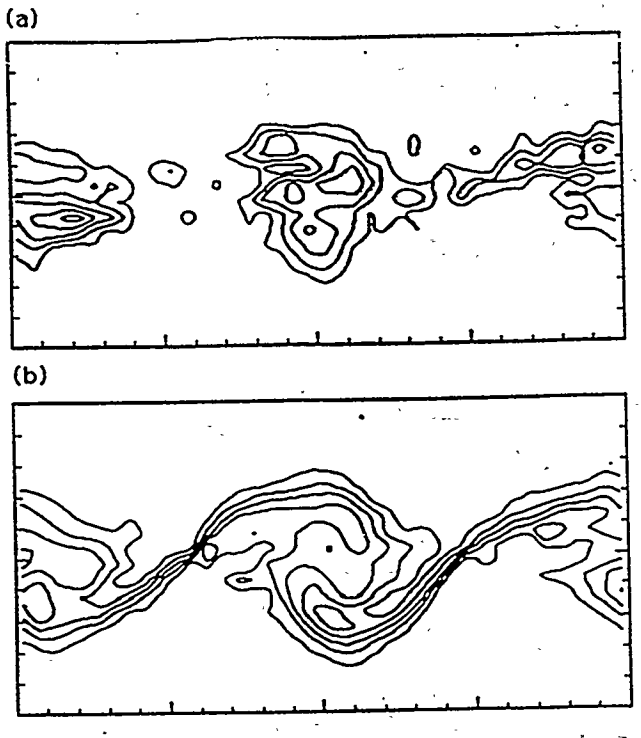

FIG. 2. Contour maps of (a) vorticity and (b) a scalar fluid marker for one realization at time $t = 25$.

This illustrates vorticity and a tracer particle trajectory contour in the mixing layer simulations of Leith (L, 90).

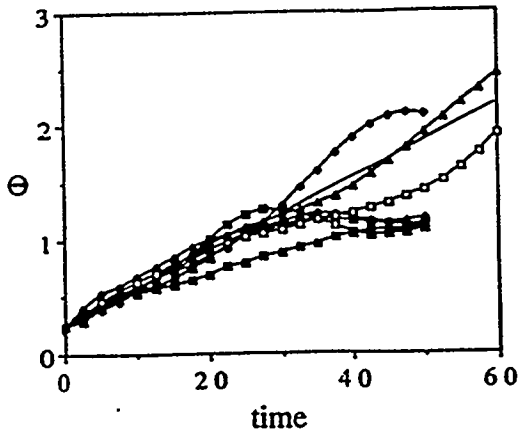

FIG. 1. Integral width Θ of the mixing layer versus time. The symbols distinguish seven independent realizations; the straight line shows the average experimental growth.

This figure eloquently illustrates the need of ensemble averaging of LES simulation realizations to develop a useful theoretical interpretation of the results, in this case mixing layer growth.

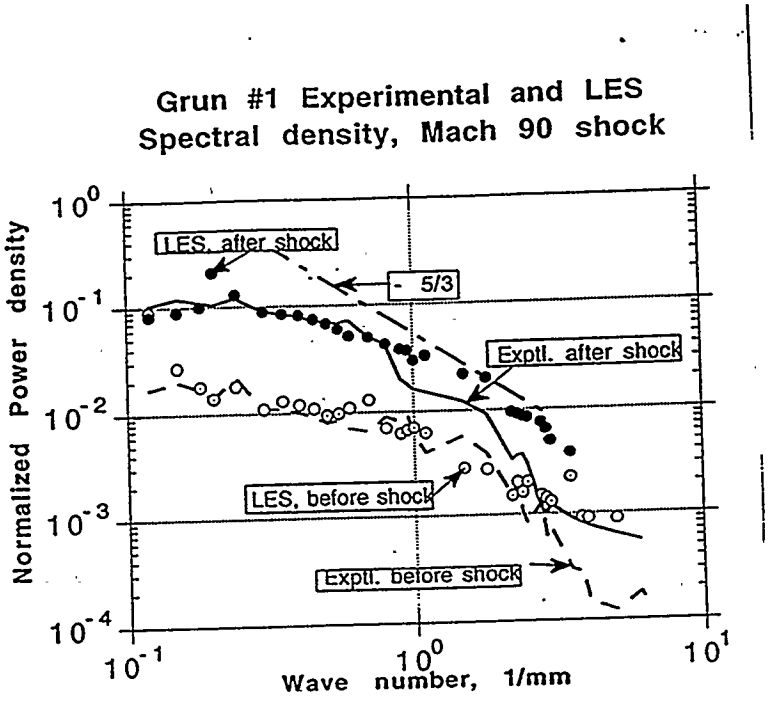

This figure indicates the progress we have made in sub-grid scale modeling for LES simulations of compressible flow with interactive shock waves. This shows the energy spectrum before and after shock passage comparing experiment with simulation results. (B-G, 93).

V. References

- Bartlett, Eugene P., Anderson, Larry W., and Kendall, Robert M. 1972, *Proc. 1972 Heat Transfer and Fluid Mechanics Institute*, eds. Raymond B. Landis and Gary J. Hordemann, Stanford Univ. Press, 262. (B-A-K, 72)

- Bird, R. Byron, Stewart, Warren E., and Lightfoot, E. N., 1960, *Transport Phenomena*, J. Wiley & Sons, NY (B-S-L,60)

- Buckingham, A. C., 1979, *AIAA 12th Fluid and Plasma Dynamics Conf., Williamsburg, VA*, AIAA Paper No. 79-1484, (B, 79)

- Buckingham, A. C., 1980, *AIAA-SAE-ASME 16th Joint Propulsion Conf., Hartford, CT*, LLNL Preprint UCRL-83727, (B, 80)

- Buckingham, Alfred C. and Siekhaus, Wigbert J., 1981, *AIAA 19th Aerospace Sciences Mtg., St. Louis, MO*, AIAA Paper No. 81-0346, (B-S, 81)

- Buckingham, A. C., 1981, *AIAA J, 19, (4)*, 501. (B, 81a)

- Buckingham, A. C., 1981, *AIAA J, 19, (11)*, 1422. (B, 81b)

- Buckingham, Alfred C. and Siekhaus, Wigbert J., 1982, *Proc. Tri-Service Symp. Gun Tube Wear & Erosion, LCWSL ARRADCOM, Dover, NJ*, LLNL Preprint UCRL-87686, (B-S, 82)

- Buckingham, Alfred C. and Hawke, Ronald S., 1982, *Proc. Tri-Service Symp. Gun Tube Wear & Erosion, LCWSL ARRADCOM, Dover, NJ*, LLNL Preprint UCRL-87857, (B-H, 82)

- Buckingham, Alfred C., Siekhaus, Wigbert J., Ellzey, Janet and Daily, John W., 1983, *Numerical Methods in Laminar and Turbulent Flow, III*, eds. C. Taylor, J. A. Johnson, and W. R. Smith, Pineridge Press, Swansea, UK, 1077 (B-S-E-D, 83)

- Buckingham, A. C., Siekhaus, W. J., Price, C. W. and Goldberg, A., 1983, *Fundamental Mechanisms of Erosion, Final Report of Research conducted under U. S. Army Contract 15812-MS (Sept. 1978 - June 1983)*, LLNL Report UCRL-53468, (B-S-P-G, 83)

- Buckingham, A. C. and Siekhaus, W. J., 1983, *Erosion by Liquid and Solid Impact*, eds J. E. Field and N. S. Corney, Cavendish Lab., Cambridge Univ. UK, 51-11. (B-S, 83)

- Buckingham, Alfred C. and Price, Clifford W., 1984, *Fundamental Mechanisms of Multi-Phase Flow Erosion/Corrosion of Solid Surfaces, Suppl. to Final Report of Research Conducted under U. S. Army Contract 15182-MS (Sept. 1978 - June 1983)*, Supplement to LLNL Report UCRL-53468, (B-P, 84)

- Buckingham, Alfred C., 1985, *Proc. 1986 Cavitation and Multiphase Flow Forum, ASME Fluids Engineering Conf., Atlanta, GA*, LLNL Preprint UCRL - 93615, (B, 85)

- Buckingham, Alfred C., 1986, *Numerical Methods for Non-Linear Problems, III*, eds. C. Taylor, D.R.J. Owen, E. Hinton, and F. B. Damjanic, Pineridge Press, Swansea UK, 883. (B, 86)

- Buckingham, Alfred C., 1987, *Proc. 1987 Winter Annual ASME Conf., Boston, MA*, LLNL Preprint UCRL-96055, (B, 87)

- Buckingham, Alfred C. and Hawke, Ronald S., 1990, *AIAA 21st Fluid Dynamics, Plasma Dynamics and Lasers Conf., Seattle, WA*, LLNL Preprint UCRL - 102303, (B-H, 90)

- Buckingham, Alfred C and Grun, Jacob, 1993, *Numerical Methods in Laminar and Turbulent Flow, VIII*, ed. C. Taylor, Pineridge Press, Swansea, U.K. 1187. **(B-G, 93)**

- Bush, William B. and Francis E. Fendell, 1977, *Turbulent Combustion, Vol. 58, Progress in Aeronautics and Astronautics*, ed. L.A. Kennedy, AIAA, NY, 3. **(B-F, 77)**

- Corner, J. , 1950, *Theory of the Interior Ballistics of Guns*, J. Wiley & Sons, Inc., NY. **(C, 50)**

- Crowe, C. T. and Pratt, D. T., 1972, "Gas-Particle Flow in Combustion Chambers", *WCSI Paper No. 72-5, Proc. Spring Mtg Western States Combustion Institute (April, 1972).* **(C-P, 72)**

- Davidson, Norman, 1962, *Statistical Mechanics*, McGraw-Hill Book Co., Inc, NY **(D,62)**

- Edelman, R. B. and Harsha, P. T., 1977, *Turbulent Combustion, Vol. 58, Progress in Aeronautics and Astronautics*, ed. L.A. Kennedy, AIAA, NY, 55. **(E-H, 77)**

- Fedyna, R., Levy, M. E., Stiefel, L., 1979, "Use of Inorganic Wear Reducing Additives to Increase 7.62 mm Barrel Life with Single-Base Extruded Propellants", U.S. Army R & D Command TR ARSCD-TR-78004, **(F-L-S, 79)**

- Gilbert, M., Davis, L., and Altman, D., 1955, *Jet Propulsion, 25*, 26. **(G-D-A, 55)**

- Hassman, H., 1970, "Review and Trends of Wear Reducing Additives in Large Calibre Tank and Artillery Cannon", *Proc. Interservice Tech. Mtg. on Gun Tube Erosion and Control*, Watervliet Arsenal, Watervliet, NY , 2.1-1 - 2.1-15 **(H, 70)**

- Hirschfelder, Joseph O., Curtiss, Charles F., and Bird, R. Byron, 1954, *Molecular Theory of Gases and Liquids*, J. Wiley & Sons, Inc., NY. **(H-C-B,54)**

- Kendall, R. M. and Bartlett, E. P., 1968, *AIAA J., 6*, (6), 1089. **(K-B, 68)**

- Leith, C. E., Jr. 1990, Phys. of Fluids A, 297. **(L, 90)**

- Mirels, H., 1956, *NACA-TN 3712*, **(M, 56)**

- Picard, J. P. and Trask, R. L., 1972, "Talc, A new Additive for Reducing Gun Barrel Erosion", Proc. Tri-Service Gun Propellant Symposium I, Picatinny Arsenal, Dover NJ, 6.2-1 - 6.2-12 **(P-T, 72)**

- Price, C. W, 1984, *Scripta Metallurgica (6)*, LLNL Preprint UCRL-90693, **(P, 84)**

- Russell, L. H., 1975, "Simplified Analysis of the Bore Surface Heat Transfer Reduction in Gun Barrels as Achieved by Using Wear-Reducing Additives", *Naval Surface Weapons Center Report NSWC/DL TR-3378*, **(R, 75)**

- Stewartson, K., 1964, *The Theory of Laminar Boundary Layers in Compressible Fluids*, Oxford at the Clarendon Press. **(S, 64)**.

- Yule, A. J., Chigier, N. A., Atakan, S., and Ungut, A., 1977, *Turbulent Combustion, Vol. 58, Progress in Aeronautics and Astronautics*, ed. L.A. Kennedy, AIAA, NY, 247. **(Y-C-A-U, 77)**